Technical University in Prague, Faculty of Nuclear and Physical Engineering

**Department of
Physics Area: Nuclear
Engineering
Focus: Experimental nuclear physics**

Spectra in pˇrˇıˇcn´e momentum and correlations from the blast wave model with resonances
Transverse momentum spectra and correlations in the blast wave model with resonances

BACHELOR´S T

Elaborated: Koˇsaˇr
Head of the study: Dr. Boris Tom´aˇsik,
Department of Physics Year: 2010

Before the wedding, instead of this page enter the assignment with the signature of the dean (will be the only two-sided letter in your country) !!!!

Prohl´aˇsen´ı

I declare that I have prepared my bachelor thesis independently and I have used only the materials (literature, projects, software, etc.) listed in the attached list.

I have no obvious reason against the use of this work within the meaning of Act No. 121/2000 Coll., on copyright law, on laws related to the copyright law and on amendments to certain laws (the Copyright Act).

In Prague on ....

....
Koˇsaˇr

Subsection

I would like to thank Dr. Boris Tom´a´sik for his excellent guidance of my Bachelor´s thesis, for his patience
and for all the time spent explaining the issues, evaluating our work and up-
I point out the mistakes and errors I have made.

The name of the work:
Spectra in pˇrˇıˇcnˊe momentum and correlations from the blast wave model with resonances

Author: Koˇsaˇr

Branch: Nuclear engineering
Type of action: Bakalˊaˇrskaprˊace

Head of the study: Dr. Boris Tomˊaˇsik, Department of Physics
                        Department of Physics, Faculty of Nuclear and Physical Engineering, Czech Technical University in Prague
Consultant: -

Abstract: Prˊace is a reˊserˊe of the theory of the behaviour of states of matter with high energy density, which is produced by the collision of three low ions at energies higher than GeV per nucleon. The book contains basic information on the extreme state of matter called the quark-gluon plasma, an into quantum statistical mechanics and an into the theory of the boost-invariant expanding fireball of hadronic matter.

The particular object of interest is the Blastwave model with included resonances, whose basic assumptions are the underlying boost-invariant expansion, the overexpansion and the existence of a specific superplane in spacetime, on which the hadronic matter is released from the fireball in a jump.

In the last part of the paper the author fits the two most important parameters of the model

Blastwave by by program DRAGON [B. Tomasik, Comp.Phys.Commun. 180 (2009) 1642-1653] on the spectra in the forward momentum obtained from the STAR experiment.

Title:

Transverse momentum spectra and correlations in the blast wave model with resonances

Author: VKoˇsaˇr

Abstract: This thesis provides a review about the basics of theories of properties of matter with high energy density, which originates in heavy ion high energy collisions (GeV/nucleus). Basic information about the extreme state of matter called quark- gluon plasma, introduction to quantum statistical mechanics and introduction to theory of longitudinally boost-invariantly expanding fireball of hot matter are men- tioned.

Particular intention is given to the blast-wave model with resonances, whose basic assumptions are longitudinally boost-invariant expansion, transverse expansion, and the existence of a particular hypersurface in space-time, on which hadronic matter abruptly decouples from fireball.

In the final part two most important parameters of the blast-wave model are extrac- ted from fits to the transverse momentum spectra obtained from STAR experiment, using a modification of the program DRAGON [B. Tomasik, Comp.Phys.Commun. 180 (2009) 1642-1653].

Table of Contents

Water

The small ion behaves roughly like a drop of liquid with pˇribliˇznˇe homogeneous goose- totality, in the rest frame pˇribliˇznˇe spherically symmetrically distributed around the body. If we observe high-energy collisions (from 1GeV per nucleon) of two three ions, even in the case of a more central entrance of the collision, there is a lower expansion due to the quan-

these phenomena - the nuclei the "sight". In the area of the pathway in the case of the are more and more heart

the nuclear liquid is strongly undergrown due to the interaction of extreme conditions - the nuclear liquid is strongly undergrown

price. If the energy density reaches the necessary values, the formation of a hypotetic quark-gluon plasma can occur. The quark phenomena cause the transfer of part of the energy of this very dense drop of nuclear matter to the formation of a particle-antiparticle pair, and the considerable pressure causes their overexpansion.

Thus, a fireball of many ˇc´asticˇc´asteˇs is created, expanding more and more substantially into space. As the fireball expands, its energy density decreases, and this causes two significant reverse transitions. First, from a quark-gluon plasma to a hadronic

Gas. This transition is called hadronization. Hadron gas is still sufficiently dense, strongly interacting, so that it can be considered as approximately thermalized.

Only there is a transition from dense hadronic gas to free hadrons. This transition is called freezing. As the fireball continues to expand, the energy density continues to decrease and the unstable particles decay. We then detect only the more stable particles and try to reconstruct from them the physics of the original nuclear core - the equations of state of the short-lived states of matter (i.e. The nature of the collective behaviour of dense nuclear matter), the laws of elementary interactions at high energies, the behaviour of a highly excited vacuum.

The question is how to choose a model to describe the high-energy interaction of two three ions and how to choose its parameters. One of the many models is the Blastwave model, whose basic assumptions are the presence of a boost-invariant expansion, an overexpansion and the existence of a specific superplane in spacetime at which the hadronic matter is released in a jump from the fireball. The author of this paper tries to find the best choice of the two main parameters of this model by means of the DRAGON program [9], which includes the effect of resonances, by fitting the spectra in the forward momentum.

Chapter 1

Contempo view of the structure rary´ masses

1.1 Element´arn´ı ˇc´astice

The elementary unit of matter is the elementary particle, which is an indivisible object with certain physical properties. Under certain circumstances, certain Sohastable structures can be divided according to the degree of elementarity into: cell, molecule, atom, shell and nucleus.

An atom is made up of a shell and a nucleus. The shell of the atom consists of electrons in an arrangement determined by electromagnetic interaction with an oppositely charged nucleus. This composed of nucleons - protons and neutrons, whose constituents are a triplet of quarks.

In the last century it has become apparent that nature is not limited to protons, neutrons and electrons, but is made up of a much larger group of particles, which are in turn made up of a relatively small group of quarks and leptons. This idea is called the standard model, which, together with quantum chromodynamics, quantum electrodynamics, where interactions are mediated by a intermediate particle, constitutes the basis of modern particle physics.

1.2 Standard model

We divide the elementary particles of the standard model into three groups - quarks, gluons and intermediate bosons. For each particle there is also a antiˇc particle, pˇriˇcemˇz in some cases the particle and the antiˇc particle are indistinguishable. We divide quarks and leptons into three generations, the first one being stable and the other two being unstable excitations decaying with weak interaction on the first generation elementary particle.

Quarks are carriers of the colour charge of the strong interaction. There are stars in

the bound
state to other quarks, so that the "set" of colours was neutral. Therefore, the quarks form the "stars" hadron: either a baryon, in which all three quarks have a different colour, or a meson, in which
which is a quark and an antiquark, i.e. a colour and its anti-colour. Theoretically, the following have been determined

and more complex structures such as the   is composed of four squares and one pentaquark, which is an antiquark.

Quarks never occur individually, but are embedded in the hadron together with other quarks. If we were to try to tear two quarks apart, their potential energy would grow linearly with their distance. The properties of the gluon, the boson that mediates the strong interaction, play a very important role here. The gluon is immaterial and has a strong interaction charge, which makes it easy to form and interact with other gluons. Eventually, as the quark is pulled away, the binding energy increases sufficiently to give rise to a quark-antiquark pair. This recombines with the original quarks that were pulled away and we have both quarks back in the bound state.

The interaction between the particles is mediated by intermediate bosons. This means, the energy and momentum are translated into quanta by intermediate bosons, which exist often very shortly, and so, due to the uncertainty principle, their mass has a certain uncertainty.

Figure 1.1: Elementary part of the Standard Model. [11]

1.3 Quark-gluon plasma

The quark-gluon plasma, abbreviated QGP, is a state of matter governed by the theory of quantum chromodynamics (QCD). The original proposition of the quark-gluon plasma is
[14]. If the matter - hadronic gas is condensed into a volume of sufficient energy density
gies [1GeVfm^{-3}], the quarks of different hadrons are close enough to each other, they are destined to be bound to their hadronic triple or pair and can
to move freely. Thus, if we can say that   shared" with each other, "the two of them have agreed

12

on a distinction."
to individual hardons becomes meaningless, then we call this state quark-gluon with plasma.

However, no theory can do without experimental facts and therefore we need a device for QGP 🔩. We expect that if the energy of two *ions of* tˇeˇzk elements is sufficiently high, we will achieve the necessary energy density for the existence of a QGP phase for a period of time
10^{-23} *p.* We call such a heart a *Little Treska*. By the nature of the QGP, it is impossible to investigate it directly, but by observing the formation of more hadrons we could learn about this
state to learn a lot. For this purpose, accelerators and particle detectors are used, which are able to measure the edge energy needed for QGP formation and can effectively observe the produced particles.

1.4 QGP and Velkyˊ tˇresk

In the large volume theory we consider the dissolution of a large amount of matter from a state of high density. If the theory is consistent with reality, the matter must have passed through the QGP state within 10μs after the onset of the Big Bang. If we can investigate this state of matter sufficiently, we will gain further insights into the origin of the universe. The problem lies in some of the differences between the *Big Bang*, from which the universe originated, and the *Little Bang*, which we can create at the accelerator:

1. *Much faster hadronization of the fireball of Malˊe tresko.*

   While for the Big Bang we assume that the expansion of the QGP fireball is slowed down by the gravitational acceleration of a huge amount of accumulated matter, for the Little Bang we assume expansion into the vacuum. We can derive the characteristic hadronization times of the QGP of the Large Tres-$_{bb}$ = 10μs and of the Small Tres-

   $\tau_{mb} = 10^{-17}\,\mu s.$

2. *Nonzero baryon force in the fireball of Malˊe tˊresko.*

   In the post-atomic universe, the baryon force was practically zero, unlike in the experimeter. The asymmetry between matter and antimatter at the acceleration
   is described by the ˇtight baryon equation $B = N_B - N_{B^-}$. Ideally
   $B = 0$. In the case of the heart, we produce ˇcˊastic-antiˇcˊastic pairs, and thus in the case of B
   the number of detected N , or at least B/N 0, increases. The problem of asymmetry can theoretically be overcome by extrapolation of the baryon chemical potential. In addition, by increasing the energy of the interface we increase the number of particles formed.

3. *Much higher energy density.*

   According to the theory of the Big Bang, the universe evolves from a continuous singularity characterized by, among other things, infinite density and temperature. By studying the accelerator we can only reach finite values.

Chapter 2

Quantum statistical mechanics

2.1 Quantum statistical mechanics

We define *the density matrix* as a self-consistent, positive operator with unit hundred.

$$\hat{\rho}^{\dagger} = \hat{\rho} \qquad \forall \, |\psi> \, \in H \; <\psi|\hat{\rho}\psi> \, \geq 0 \qquad \mathrm{Tr}\,\hat{\rho} = 1$$

The density matrix can be defined using the positive terms w_j and the vector $|\psi_j> \, \in H$ next:

$$\hat{W} = \sum_j w_j \frac{|\psi_j><\psi_j|}{<\psi_j|\psi_j>} \qquad \hat{\rho} = \frac{\hat{W}}{\mathrm{Tr}\,\hat{W}}. \qquad (2.1)$$

Therefore, using the density matrix we can also calculate the *mean value of the observable* $\bar{O} = \hat{O}$:

$$\bar{O} = \sum_j w_j \frac{<\psi_j|\hat{O}\psi_j>}{<\psi_j|\psi_j>} = \mathrm{Tr}[\hat{\rho}\hat{O}].$$

In this example we will use the natural units $n = c = k_B = 1$.

2.2 The truest difference between the Grandkano-nicky´ file

Whether we have   a system that   is described by two commuting operators quantum

$\hat{H}, \hat{B}$ i.e. hamiltonian and baryon ˇc´ısle. Since we will be working with general states and not just the eigenstates of the baryon force operator, we will actually build a grand canonical statistical ensemble where the baryon force is not fixed.

Let the Hamiltonian have a discrete spectrum $\hat{H}\hat{P}_j = E_j\hat{P}_j$ where $\hat{P}_j$ is an orthogonal projector onto the proper subspace. Let us define the common set of orthogonal projectors on their own subspaces $\{\hat{P}_l \mid \hat{H}\hat{P}_l = E_l\hat{P}_l \wedge \hat{B}\hat{P}_l = b_l\hat{P}_l\}$

Let us now consider a statistical ensemble of states with different values of the baryon pressure and energy, which we describe by means of the density matrix:

$$\hat{\rho} = \sum_l w_l \frac{\hat{P}_l}{\mathrm{Tr}\,\hat{P}_l},$$

where p´ad´ad´ame assumes that $\dim \hat{P}_l = \mathrm{Tr}\,\hat{P}_l < +\infty$.

The mean values of the energy $\bar{E}$ and the baryon $\bar{b}$ are known:

$$\bar{E} = \mathrm{Tr}[\hat{\rho}\hat{H}] = \sum_l w_l E_l \qquad \wedge \qquad \bar{b} = \mathrm{Tr}[\hat{\rho}\hat{B}] = \sum_l w_l b_l.$$

Položme si nyn´ı otázku jaká je nejpravděpodobnější matice hustoty, či ekvivalentně jaké je nejpravděpodobnější rozdělení nalezen´ı různých hodnot energie a baryonového čísla. Zavedeme entropii:

$$S = -\mathrm{Tr}[\hat{\rho}\ln\hat{\rho}] = -\sum_l w_l \ln w_l$$

and we will maximize it for the given conditions, for $\bar{E},\ \bar{b}$.

$$\Lambda(w_1, w_2, \ldots) = -\sum_l w_l \ln(w_l) + \alpha \sum_l w_l - \beta \sum_l w_l E_l + \ln\lambda \sum_l w_l b_l, \qquad (2.2)$$

where β, $\ln\lambda$ are Lagranger multipliers. Sometimes we refer to $e^{\beta\mu} = \lambda$ as the fugacity, where μ is the baryon chemical potential.

Let us look for an option w_j so that the function $\Lambda(w_1, w_2, \ldots)$ has a maximum in it. Because

$$\nabla^2 \Lambda(w_1, w_2, \ldots) = -\sum_l \frac{1}{w_l} < 0 \text{ on } w_l \in (0, 1)$$

lies the maximum at the stationary point of the function - i.e. at the point where w_l is satisfied:

$$\forall l\, \partial_{w_l}\Lambda = 0.$$

We're getting a lot out of it:

$$w_l = Z_G^{-1} e^{-\beta(E_l - \mu b_l)} = \langle l | Z_G^{-1} e^{-\beta(\hat{E} - \mu\hat{B})} | l \rangle,$$
$$\text{where } Z_G = e^{\alpha^{-1}} = \sum_l e^{-\beta(E_l - \mu b_l)} \text{ is called the partition function.}$$

16

And so we have
enough:

$$\bar{E} = -\partial_\beta \ln Z_G \qquad \bar{B} = -\frac{1}{\beta}\partial_\mu \ln Z_G.$$ (2.3)

For the density matrix in this state we have:

$$\hat{\rho} = \frac{e^{-\beta(\hat{H}-\mu\hat{B})}}{\text{Tr}\, e^{-\beta(\hat{H}-\mu\hat{B})}}.$$

For the partition function
we have:

$$Z_G = \text{Tr}\, e^{-\beta(\hat{H}-\mu\hat{B})} = \sum_n <n|\, e^{-\beta(\hat{H}-\mu\hat{B})}\,|n>.$$ (2.4)

Since Tr is representationally invariant, we can use any ortho-normal basis. This allows us to learn a base of occupation rules for non-interacting. The interaction is then sometimes introduced by means of a disturbance development.

2.2.1 Bosons and fermions

Consider a system of indistinguishable and noninteracting particles described by two commuting operators, the Hamiltonian $\hat{H}$ and the baryon operator $\hat{B}$. Let the single-valued hamiltonian $\hat{H}_{(1)}$ be only discrete values $\hat{H}_{(1)}|j> = E_j|j>$, where $|j>$ is an eigenvector. We introduce a symmetrized or antisymmetrized basis on the Fock space containing of scientific words:

$$\{|(S/A), n_1^{(b_1)}, n_2^{(b_2)}, n_3^{(b_3)} ... >,$$

where $n_i^{(b_i)}$ are the occupation numbers of the single-variable states $|i>$,

for which $\hat{H}_{(1)}|i> = E_j|i> \wedge \hat{B}|i> = b_i|i>\}.$

For the total Hamiltonian (Fock space) and baryon space we get:

$$\hat{H}|(S/A), n_1^{(b_1)}, n_2^{(b_2)}, n_3^{(b_3)}... > = \sum_i n_i^{(b_i)}E_i|(S/A), n_1^{(b_1)}, n_2^{(b_2)}, n_3^{(b_3)}... >,$$

$$\hat{B}|(S/A), n_1^{(b_1)}, n_2^{(b_2)}, n_3^{(b_3)}... > = \sum_i n_i^{(b_i)}b_i|(S/A), n_1^{(b_1)}, n_2^{(b_2)}, n_3^{(b_3)}... > .$$

For the construction of the grand canonical ensemble we use the we have in us formula (2.4), which has the following form:

$$Z_G = \sum_n e^{-\sum_{i=1}^{\infty} n_i\beta(e_i - \mu b_i)} = \sum_n \prod_i e^{-n_i\beta(e_i - \mu b_i)}.$$

Because all combinations of the occupation clauses remain (if formally) contained, we can change the order of the sum and product. We draw all states with free N total number of particles.

$$FROM_G = \begin{cases} \prod_i \sum_{n_i=0}^{\infty} e^{-n_i\beta(e_i-\mu b_i)} & \text{for bosons.} \\ \prod_i \sum_{n_i=0}^{1} e^{-n_i\beta(e_i-\mu b_i)} & \text{for fermions.} \end{cases}$$

We add sums (for bosons under the condition $e^{-n_i\beta(e_i-\mu b_i)} < 1$)

$$\ln Z^{(G)}_{F^+,B^-} = \pm \sum_i \ln(1 \pm e^{-\beta(e_i-\mu b_i)}), \tag{2.5}$$

where the sum is the sum of all single-particle states, the upper sign is for fermions and the lower for bosons.

For the mean value of the baryon force from (2.3) we have:

$$\bar{B} = -\frac{1}{\beta}\partial_\mu \ln Z^{(G)}_{F^+,B^-} = \sum_i \frac{Would}{1 \mp e^{\beta(e_i-\mu b_i)}} \tag{2.6}$$

Odsud máme také Bose-Eistainovo a Fermi-Diracovo rozdělení $\frac{1}{e^{\beta(E_i-\mu b_i)}\mp 1}$. Rozdělíme-if the sum in (2.5) is divided into states with $b_i > 0$ and states with $b_i < 0$ (antičˇastic) and we assume-

if the possible states for the particles and antiparticles are the same, we get:

$$\ln Z^{(G)}_{F^+,B^-} = \pm \sum_i \left[\ln(1 \pm e^{-\beta(e_i-\mu b_i)}) + \ln(1 \pm e^{-\beta(e_i+\mu b_i)})\right], \tag{2.7}$$

where the sum $\sum_i$ will now denote the sum of all states with $b_i > 0$. Using $\lambda^{b_i} = e^{\beta\mu b_i} = e^{\mu}$ we could modify the previous relation to:

$$\ln Z^{(G)}_{F^+,B^-} = \pm \sum_i \left[\ln(1 \pm \lambda^{b_i} e^{-\beta e_i}) + \ln(1 \pm \lambda^{-b_i} e^{-\beta e_i})\right]. \tag{2.8}$$

By replacing the baryon equation by a lepton equation, we could use the same procedure to derive the equations for leptons. By allowing only the state $b_i = 1$ we obtain a system of ˇcˊastics and antiˇcˊastics of the same type.

2.2.2   Density of states

We consider a quantum mechanical with an ˇcˊasticity in an infinitely deep potential well - a box $< 0, L > \times < 0, L > \times < 0, L >$. We introduce periodic boundary conditions (on the circle), which allow for transparent shading and later

in the limit $V \to \infty$, certain boundary conditions will not be essential.

$$\psi(x_i = 0) = \psi(x_i = L)$$

We obtain a periodic wave of similar shape to the de Broglie wave, but the momentum we now have quantum The "fineness" of the quantum channel is determined annihilation: primarily by the size of the box. We have

$$\psi(x) = e^{ip\sim\sim x}$$

$$\vec{p} = \frac{2\pi}{L}(k_1, k_2, k_3) \text{ where } k_i \in \mathbb{Z}.$$

Let f be a real function of a real variable, E_n are real numbers. Let us consider the sum of

$$\sum_{n=0}^{\infty} f(E_n) = \int_0^{\infty} d\mu_D(E) f(E),$$

where in the integral we generate the measure next:

$$d\mu_D(E) = d \sum_{n=0}^{\infty} \theta(E - E_n).$$

The measure therefore determines how many E_n there are at a given point E. If the function g exists simply, with a continuous non-zero first derivative g^n on $< 0, +\infty >$ such that it appropriately approximates Trend E_n. So, for example:

$$\forall n \in \mathbb{N}_0 \quad |g(n) - E_n| < \delta_1 \quad \wedge \quad \forall x \in < n-1, n > : |g^n(x) - (g(n) - g(n-1))| < \delta_2,$$

where $\delta_{1,2} > 0$ are sufficiently small. The function can be set to $< 0, +\infty >$ invert and approximate the measure in the previous integral:

$$d\mu_D(E) \approx d(g^{-1}(E))$$

$$\sum_{n=0}^{\infty} f(E_n) \approx \int_0^{\infty} d(g^{-1}(E)) f(E) = \int_0^{\infty} dE \frac{dg^{-1}(E)}{dE} f(E).$$

The preceding procedure can be easily generalized to the following higher-dimensional variant:

$$\sum_{k_1, k_2, k_3 = -\infty}^{+\infty} f(E(\vec{p}(k_1, k_2, k_3))) \approx \int_{\mathbb{R}^3} dk_1\, dk_2\, dk_3\, f(E(\vec{p}(k_1, k_2, k_3))) = \int_{\mathbb{R}^3} d^3 p\, J\, f((E(\vec{p})),$$

where J is a suitable Jacobian. In the case of a boxed crystal $J = V/(2\pi)^3$. To simplify the procedure, we work with the integral instead of the sum, which is motivated by the fact that in the limit $L \to \infty$ the spectrum of the momentum operator is continuous. We replace the sum of the procedure by the integral of the following:

$$\sum_i [\dots] = g \int \frac{V d^3 p}{(2\pi)^3} [\dots], \tag{2.9}$$

where, in addition, we generally use the degeneracy factor g, which denotes further degrees of freedom to expand the phase space into further dimensions. We have derived this for periodic boundary conditions or arbitrarily large volumes.

2.2.3 Fermi and Bose ˇcˊastic and antiˇcˊastic gases of one type

By allowing the state with baryon ˇcˊıcˊıs only $b_i = \pm 1$ in (2.8), we derive the relation for

$\ln Z_{F^+,B^-}^{(G)}$ for ˘c´astic and $anti$˘c´astic gas of one type. If we continue with (2.9), we get mute:

$$\ln Z_{F/B}\ (V,\ \beta,\ \lambda) = \pm gV \int \frac{d^3 p}{(2\pi)^3} \left[\ln(1 \pm \lambda\ e^{-\beta\sqrt{p^2+m^2}}) + \ln(1 \pm \lambda^{-1} e^{-\beta\sqrt{p^2+m^2}}) \right],$$
(2.10)

where the upper sign is valid for fermions, the lower for bosons and the ˘c´ast at λ^{-1} corresponds to anti˘c´asticity.

Using the relation for the grand canonical potential:

$$\Omega(T,\ V,\ \mu) = -PV = -\beta^{-1} \ln Z_G,$$

where P is the pressure, we get:

$$P(\beta,\ \lambda) = \mp g \int \frac{d^3 p}{(2\pi)^3} [\ln(1 \pm \lambda\ e^{-\beta\sqrt{p^2+m^2}}) + \ln(1 \pm \lambda^{-1} e^{-\beta\sqrt{p^2+m^2}})],$$
(2.11)

where g is the degeneracy factor, see the conclusion of subsection 2.9, and where the upper sign is valid for fermions, the lower for bosons, and the ˘c´ast u λ^{-1} corresponds to antiparticles.

2.2.4 Photon gas

For the photon gas, we can derive a simple equation of state from (2.11), which corresponds to the theory of blackbody radiation. For the photon gas: $m = 0$, $E_i = p$, v We omit the integral with the frequency multiplied by λ^{-1} over the antiphoton frequency and set $\lambda^{bi} = 1$. The last two assumptions are justified by the fact that the photon and the antiphoton are indistinguishable

Therefore, the addition of a photon can be interpreted as the addition of an antiphoton, so the chemical potential can be considered as zero. for the antiparticle states disappears also due to the indistinguishability. Therefore, by substituting the assumptions into (2.11), switching to spherical coordinates, and introducing the substitution $x = p/T$ we obtain the equation of state of the photon gas:

$$P = - \frac{4\pi g T^4}{(2\pi)^3} \int_0^\infty dx\, x^2 \ln(1 - e^{-x}).$$

Because the integral is equal to $-\pi^4/45$ we get:

$$P = g \frac{\pi^2}{90} T^4,$$
(2.12)

where for photons $g = 2$ (polarization). D´ıky of the relation resulting from the definitions:

$$E(T) = -\partial_\beta \ln Z_G = -\partial_\beta - \beta PV = 3PV$$

Thus, we obtain a relation for the pressure of the radiation (the ultrarelativistic limit for the libolic frequency, i.e. for $p >> m$):

$$P = E(T)/3,$$

where $E(T)$ is the energy density of the electromagnetic field. From here we can easily determine the well-known Stefan-Boltzmann constant.

2.2.5 Bag model

The original contribution to this model is [12]. The bag model is a primitive model of the QGP hadronization process. Since we are working with high energies, we can
to neglect the masses of all QGP and HG (Hadron Gas) particles due to their Momentum. However, the degeneracy factor is a higher value, which multiplies the dimension of the phase space. We take it the phase space of fermions is somewhat smaller than that of bosons due to the Pauli exclusion principle. More precisely, 7/8 times smaller. This is shown in [5] where this example is taken from.

$$g_{QGP} = g_G + \frac{7}{8} \times 2(\text{anti\v{c}\'{a}stice}) \times g_q + g_{EW} \approx 56.5 \,,$$

where for the gluons, the quarks:

$$g_G = 2(\text{spin}) \times (N_c^2 - 1)(\text{color}) = 16 \,,$$

$$g_q = 2(\text{spin}) \times N_c (\text{color}) \times n_f \approx 15 \,,$$

$$g_{EW} = 2(\gamma) + \frac{7}{8} \times 2(\text{anti\v{c}\'{a}stice}) \times (2(\text{spin}) \times 2(e + \mu) + 3(\nu_{e_{Lv}} \mu_{Lv} \tau_L)) = 14.25.$$

We're replanting: $N_c = 3$ (number of colors), n_f 2.5 (effective number of waves). For ν, we only consider left-handed neutrinos and right-handed antineutrinos and do not assume tau production.

We estimate the hadronic gas in the zero point by the pion gas and add the electroweak particles:

$$g_{HG} = 3(\pi^+ \, \pi^- \, \pi^0) + g_{EW} \approx 17.25.$$

During hadronization, both HG and QGP pressures are equal, therefore:

$$P_H = g_{QGP} \frac{\pi^2}{90} T_H^4 - B = g_{HG} \frac{\pi^2}{90} T_H^4. \qquad (2.13)$$

From the pressure for the photon gas modelling the QGP we subtract the so-called bag constant
$B^{\frac{1}{4}} \approx 190 \text{MeV}$ obtained by fitting the experimental data, this constant is re-represents the latent heat of QGP. If we did not introduce this constant, then the stars would
$P_{QGP} > P_{HG}$ would be valid and matter would be constantly in a quark-gluon plasma state. We can also think of the constant B as the pressure that pushes the physical vacuum to

proton and hold it together." We thus estimate the temperature of hadronization:

$$T_H = B^{\frac{1}{4}} \left(\frac{1}{9\sigma^2 \Delta g} \right)^{\frac{1}{4}} \approx 130 \text{MeV}.$$

Another possibility to determine T_H is to use the formula for the radiation pressure (ultra-relativistic limit) and the energy density:

$$P = \frac{E}{3}.$$

Since the proton is the most abundant quark system, we can estimate the energy density at hadro-nization as:

$$E_H = \frac{m_p}{(1\text{fm})^3} \equiv 1\text{GeVfm}^{-3}.$$

Then, by substituting the energy density into the Boltzmann relation, we obtain the pressure with which we can estimate the hadronization temperature:

$$T_H = 160\text{MeV}.$$

Chapter 3

Sub-black boost-invariant expanding fireball

3.1 Notes

1. I use formulas in the text:

$$\delta(f(x)) = \frac{\delta(x - x_i)}{|f'(x_i)|}_i \quad \text{where the sum of b\v{e}\v{z}´ı p\v{} res points where f(x) is zero} \tag{3.1}$$

and markings:

$$\delta^+(f(x)) = \theta(x)\delta(f(x)) \tag{3.2}$$

2. For the \v{}cty\v{}r vector, we often denote by $a^\mu = a$, without emphasis, that it is a \v{}cty\v{}r vector. However, I use the symbols a_μ and $^\mu = a^2$. Three-dimensional vectors are denoted by a

3. A used formula for the fourth-order stability is:

$$p^2 = E^2 - \vec{p}^2 = m^2 \tag{3.3}$$

therefore for the following defined Dp

$$Dp = 2\delta^+(p_\mu p^\mu - m^2)d^4 p = \frac{d^3 p}{E} \tag{3.4}$$

3.2 Coordinates

3.2.1 Spatiotemporal coordinates

The following coordinates are suitable for describing the sub-black boost invariant expansion:

Let us define the super-surface on which we define the frost. We leave it as a general superplane in the fourth space. In the Blastwave model we then introduce a more

specific definition.

Above the surface of the frost:

$$\sigma = \{x^\mu \mid \text{superplane in 4-dimensional space}\} \tag{3.5}$$

But we will introduce quantities that we will use to describe the individual frequencies of the expanding fireball in the laboratory system.

Spatial vector of the fourth part of the fireball in the laboratory system:

$$x^\mu = (t, x, y, z) = (t, \vec{x}) \tag{3.6}$$

Velocity of the expelling fireball with positional x^μ:

$$U^\mu = \frac{dx^\mu}{d\tau} = J \frac{(V_0, \vec{V})}{1 - V^0 - \vec{V}}. \tag{3.7}$$

3.2.2 Co-ordinates of the ˇcˊastice

For the description of a particle in a laboratory system we define the following values:

ˊasticity:

$$p^\mu = (p^0, \vec{p}) \tag{3.8}$$

The speed of the
acceleration is inferior:

$$y = \frac{1}{2}\ln \frac{p^0 + p_z}{p_0 - p_z} \tag{3.9}$$

Velocity of the particle in the laboratory system

$$\vec{v} = \frac{\vec{p}}{p_0} \tag{3.10}$$

Vector of the pˇrˊ ıˊıcˊıcˊıcˊı
momentum of the axis:

$$\vec{p} = (p_x, p_y) = p_t (\cos \varphi, \sin \varphi) \tag{3.11}$$

Pˇrˊıˇcˊıcˊıcˊı mass of the asterisk:

$$m_t = \sqrt{Jm^2 + p_t^2} \tag{3.12}$$

Energy of the particle in the laboratory system:

$$E = p^0 = \sqrt{Jm^2 + p_2} = \sqrt{Jm^2 + p_t^2 + p_z^2} \tag{3.13}$$

Energy of a particle in the local system x^μ:

$$E^* = \sqrt{\frac{1}{1 - V^2}}(p^0 - \vec{V}) \tag{3.14}$$

We can easily see that it
pays:

$$p^\mu = (m_t \cosh y, \, p_t \cos \varphi, \, p_t \sin \varphi, \, m_t \sinh y), \qquad (3.15)$$

$$E^* = p_\mu \, u^\mu . \qquad (3.16)$$

3.3 Hydrodynamic description of the relativistic relation

In the hydrodynamic description of the relativistic relation, we introduce the following signs:

Density of the number of ˇc´astic:

$$n(\vec{x},t)d^3x = n(x^\mu)d^3x = \text{poˇcet ˇc´astic v volume } d^3x \text{ v ˇcase } t. \tag{3.17}$$

The total number of ˇc´astics in ˇcase t:

$$N^{(t=kost)} = \int d^3x\, n(x^\mu) \tag{3.18}$$

In general, we do not have to restrict ourselves to a superplane in spacetime defined by some value of time, but we can determine the number of worlds passing through a general superplane in spacetime. This must be carried out in a more complex way. This is usually done in some models of relativistic relations, where we define a freezing superplane, which we then integrate over. On this topic, see also Subsection 3.5.

Current ˇc´astic:

$$\vec{j}(\vec{x},t) = \vec{j}(x^\mu) \tag{3.19}$$

is a vector such that for any infinitesimal element of the surface dS - at the point $\vec{x}$ gives the scalar product $d\vec{x}\cdot\vec{j}(\vec{x},t)$ of the number of particles passing through the given element in time dt.

Čtyř

$$j^\mu = (n(\vec{x},t), \vec{j}(\vec{x},t)) \tag{3.20}$$

distribution of ˇc´astic:

$f(x^\mu, p^\mu)d^3x\,d^3p$ = the number of particles in the phase volume $d^3x\,d^3p$ at the point (x^μ, p^μ) (3.21) follows from here:

$$n(x^\mu) = \int d^3p\, f(x^\mu, p^\mu), \tag{3.22}$$

$$\vec{j}(x^\mu) = \int d^3p\, \vec{v} f(x^\mu, p^\mu). \tag{3.23}$$

Because the particles are located on the mass shell - i.e. $p^0 = \sqrt{p^2 + m^2} = E$, it follows from here by using (3.4):

$$j^\nu(x^\mu) = \int_{p0=E} d^3p\, \frac{p^\nu}{p0} f(x^\mu, p^\mu) = \int Dp\, p^\nu f(x^\mu, p^\mu). \tag{3.24}$$

Henceforth, however,
for $p^0 = E$:

$$E\frac{d3 j^\nu}{d3p}(x^\mu, p) = p^\nu f_{(x^\mu\ p^\mu)}, \tag{3.25}$$

$$E\frac{d3 N^{(t=bone)}}{d3p}(t, p) = \int d^3x\, E f_{(x^\mu\ p^\mu)}. \tag{3.26}$$

However, the previous formula is valid only for the integration over the

spacetime plane from constant time. More generally, the worlds are calculated and the procedure is more complex. See Section 3.5.

3.3.1 Differences in the axis

For the description of the difference of particles in spacetime we use the Lorentzian invariant difference, which is a generalization of the non-relativistic difference, which is invariant under the Galilean transformation. This satisfies the requirement that the higher transformed momentum spectrum corresponds in all systems to a higher invariant representing the frequency of the particle energy in a given system, i.e. $p2 + {}^{m2}$. The invariance is easily obtained by trans- forming the differential equation of the component of the uncertainty p and by applying the modified formula for the energy. The total number of particles on the chosen space-time superplane is N.

Lorentz invariant distribution:

$$N\frac{d^3 E}{d3p} = p_0 \frac{d^3 N}{d3p} = \sqrt{p2 + {}^{m2}} \frac{d^3 N}{d3p}(p) \tag{3.27}$$

Production function:

$$S(x, p) \quad \text{such that} \quad E\frac{d^3 N}{d3p} = \int d^4 x\, S(x, p) \tag{3.28}$$

Local Boltzmann difference:

$$f(x^\mu, p) = \frac{d3jo}{d3p} \propto n(x^\mu) \exp(-E^*/T), \tag{3.29}$$

where E^* is replaced by (3.14).

3.4 Bjorken's boost invariant expansion

At very high energies, we can use the phenomenological model of a divergent invariant expansion, in which the separation of the produced particles with a given rapidity is approximately uniform in the region between the rapidities of the original particles y_0. [2] i.e:

$$\frac{dN_B}{Always} = \begin{cases} N^{-1} & y \in < -y_0, y_0 > \\ 0 & \text{otherwise.} \end{cases}$$

As a consequence, in the limit of $y_0 \to \infty$ the expansion (even too high) occurs in the same way in each system of the set of systems mutually boosted, i.e. in each such system the difference has the shape given by the relation. The only problem with which we have to deal with is the finality of y_0. We can assume that for boosts in the „small" region of medium rapidity $y = 0$ we approximately achieve uniformity.

3.5 Differences in momentum during freezing

The original work concerning this subsection is [1]. We assume that freezing occurs in every system in the same *sub-black proper case*, i.e. at $\tau = \tau_{fo}$. Thus, we do not consider the contribution to the *eigentime* due to the *boost-invariant* expansion, which is consistent with the *boost-invariant* expansion *of the fireball*.

Intuitively, we would assume that in order to obtain the difference between the particles, it is sufficient to integrate the invariant difference over the *freezing surface* (3.43):

$$E\frac{d^3 N}{d3p} = \int_\sigma E^* f\, ,p^\nu) = \int_\sigma at_\mu\, f\, ,p^\nu),$$
$$(x^\nu \qquad p^\mu\ (x^\nu$$

but this assumption is wrong. Such a definition would violate the law of conservation of energy. This can be proved after the integration of EdN. [1].

Let us define an element of a superplane as a vector which has a norm equal to the surface of the superplane and is a quartic perpendicular to it:

$$d\sigma_\mu = \varepsilon_{\mu\nu\nu_1\nu_2\nu_3}\, \partial_\alpha x^{\nu_1}\, \partial_\beta x^{\nu_2}\, \partial_\gamma x^{\nu_3}\, d\alpha d\beta d\gamma,$$

where α, β, γ are the coordinates used to parameterize the superplane. Consider now the number of worlds that intersect the hyperplane σ at point x^μ and have momentum close to p^μ:

$$dN(\sigma, x^\mu,\ ) = f\ ,\ )d\sigma_\mu\quad)p^\mu Dp = d\sigma_\mu\ )\frac{d3j\mu}{d3p}(x^\nu,)d^3 p, \qquad (3.30)$$
$$p^\mu\ (x^\mu \quad p^\mu\ (x^\mu \qquad (x^\mu$$

where Dp comes from (3.4) and the second equality follows from (3.25).
meets the requirements of the theorem, let us discuss two choices of hyperplane:

$$d\sigma^{(t=kost)}_\mu = (0, 0, -dxdydt), \qquad d\sigma^{(t=kost)}_\mu = (dxdydz, 0, 0, 0).$$

$$dxdydz\, d^{3n}(x^\nu,)d^3 p = \quad \text{number of particles in the phase volume } d^3 x d^3 p$$

$$dN = \qquad \overline{d3}$$

$$dxdydt\frac{p}{d3p}(x^\nu,)d p^3 = \text{the number of particles, which flow through the area}$$
$$\qquad\qquad dxdy$$
$$\frac{d^3}{j_3} \qquad\qquad \text{for } \check{\ }\text{cas } dt \text{ and } p^n \in (p \pm dp).$$

From here we can easily go to the general form of the decomposition $d\sigma_\mu = c_\nu\, d\sigma^{(x^\nu = const)}_\mu$ where $c_\nu c^\nu = 1$ determines the unit normal to the hyperplane at point x^β. Ov˘e˘rme:

$$d\sigma_\mu p^\mu = [c_\mu p^\mu]d\sigma = c^\nu [n^{(\nu)}_\mu p^\mu]d\sigma = c_\nu \sum_\nu [d\sigma^{(x^\nu = kost)}_\mu p_\mu],$$

where $n^{(\nu)}$ are unit vectors in the direction of the ν axes. This verified that (3.30) is the number of worlds that intersect the hyperplane σ at point x^μ and have momentum close to p^μ.

Let's now modify the formula for dN into the form of an invariant distribution by applying the formula for Dp
(3.4) and for the second equality (3.25) and we get:

$$E\frac{d3N^{(\sigma)}}{d3p} = \int_\sigma d\sigma_\mu\, f\ ,p^\nu)\ \int_\sigma d\sigma_\mu\frac{d3j\mu}{d3p}(x^\nu,). \qquad (3.31)$$
$$p^\mu\ (x^\nu =$$

For the production function (3.28) we get:

$$S(x, p)d^4 x = d\sigma_\mu (x)p^\mu f (x, p).$$

(3.32)

3.6 Symmetrization of the production function, parameterization

We will now review the theory of the effect of symmetrization for indistinguishable bosons on their pro-duction functions, but we will not further investigate the data related to this part.

Due to the properties of indistinguishable particles, the amplitude A_N of the production of particles is symmetric or antisymmetric in the momenta of the produced particles. Let us consider the amplitude of the production of an N-˘c´astic system with momenta p^μ arising at five points x^μ_i, where $i \in \{1, 2 \ldots N\}$. Then due to symmetry and antisymmetry, respectively, the truth of the formation of a system of particles with momenta p^μ_i in the region G of the following:

$$A_N(p^\mu_i, G) = \int_G d^{3N}x \sum_{\pi \in S_n} \text{sgn}\,\pi\, A e\left((p^\mu_{\pi(1)}, x^\mu_1), (p^\mu_{\pi(2)}, x^\mu_2) - - - (p^\mu_{\pi(N)}, x^\mu_N)\right),$$

$$P_N(p^\mu_i, G) = A_N(p^\mu_i, G)^2,$$

where for bosons we consider $\text{sgn}\,\pi = 1$ and for fermions $\text{sgn}\,\pi$ is the sign of the permutation.

The effect of symmetrization turns out to be for a small region G and it had different momentum in ˘r´ades $\Delta p \Delta x \eta$. We can investigate this effect for the two-variable axis by introducing a correlation function:

$$c(p^\mu_1, p^\mu_2) = \frac{P_2(p_1^\mu, p_2^\mu)}{P_1(p^\mu_1) P_1(p^\mu_2)} = \frac{E_1 E_2 \frac{d^6 N}{d^3p_1 d^3p_2}}{E_1 \frac{d^3N}{d^3p} E_2 \frac{d^3N}{d^3p}}. \tag{3.33}$$

If we calculate the single-variable spectrum using the production function (3.32), we can derive [6, 7]

$$c(p^\mu_1, p^\mu_2) = 1 + \frac{|\int d^4x\, S(x,K)\exp(iqx)|^2}{E_1 \frac{d^3N}{d^3p} E_2 \frac{d^3N}{d^3p}} = 1 + \frac{|\int d^4x\, S(x,K)\exp(iqx)|^2}{\int d^4x\, S(x,p_1)\int d^4y\, S(y,p_2)}, \tag{3.34}$$

where $q = p_1 - p_2$ and $K = \frac{p_1+p_2}{2}$. We take the so-called smoothness approximation: $p_1 \approx p_2 \approx K$ and proceed to the new coordinates:

$$c(p_1, p_2) - 1 = C(q, K) - 1 \approx \frac{|\int d^4x\, S(x,K)\exp(iqx)|^2}{(\int d^4x\, S(x,K))^2},$$

where $c(p_1, p_2) = C(p_1 - p_2, \frac{p_1+p_2}{2})$.

3.6.1   N´astin derivation of the symmetrization effect

I was inspired by the work [8]. The derivation of the symmetrization effect can be suggested as follows:

The amplitude of the production can be thought of as a simple wave function of the trajectory and the formation of the trajectory as a measurement on this function.

Univariate production function

Let us consider a point source, in which a particle in the eigenstate of the momentum operator with a difference $r(p)$ with a p h a s e $\varphi(x_1)$ at the point x_1 independent of its impulse can arise. The position of the phase at a certain point is an essential element of this model, because it provides a kind of minimal localization of the origin of an otherwise delocalized de Broglie wave, which we will see later - when centred, it will have a significant effect. In the x-representation we h a v e :

$$< x|\psi > = \int dp\, r(p)\, e^{ip(x - x_1)}\, e^{i\varphi(x_1)}.$$

This can be interpreted as an approximation of the production of a particle a r i s i n g at a point x_1 with the s t a t e p h a s e $\varphi(x_1)$ in the x-representation. Let us now consider a m o r e g e n e r a l source in the pulse with a slowly v a r y i n g difference function $S = |a(x, p)|2$, where $a(x, p)$ is the amplitude:

$$< x|\psi > = \int dp \int dx^{\prime}\, a(x^{\prime}, p)\, e^{ip(x - x^{\prime})}\, e^{i\varphi(x^{\prime})}.$$

We can easily move to a p-representation that is m o r e i n t u i t i v e from the point of view of our production
with a certain momentum, therefore we denote $A(p)$:

$$A(p) = < p|\psi > = \int dx^{\prime}\, a(x^{\prime}, p)\, e^{-ipx^{\prime}}\, e^{i\varphi(x^{\prime})}.$$

Here we can of course satisfy the locality of the particle by e.g. an exponential ball around the distributed momentum and later on we c a n i m p r o v e the smoothness of the distribution function and thus obtain the same

We h a v e squared absolute values and usually a centred plot of a finite time interval. Since there is no reason to prefer a different phase at any point, we will center this quadrant j e ˇ s t ˇ e on all choices of the phase function at all points of production:

$$|A(p)|2 = \int dx^{\prime} \int dx^{\prime\prime}\, a(x^{\prime}, p)\overline{a(x^{\prime\prime}, p)}\, e^{-ip(x^{\prime} - x^{\prime\prime})}\, e^{i(\varphi(x^{\prime}) - \varphi(x^{\prime\prime}))}.$$

Let us f o r m a l l y reduce the expression of all functions $\varphi(x)$: $< _{\bot} + > < \pi, +\pi >$ to a fraction of the previous integral:

$$\int_{\{\varphi(x)\}} d\varphi\, e^{i(\varphi(x^{\prime}) - \varphi(x^{\prime\prime}))} = \delta(x^{\prime} - x^{\prime\prime}).$$

The validity of this relation can be formally v e r i f i e d by discretizing the problem or by s t a t i n g the similarity with the Feynmann integral for the propagator of the system, whose lagrangian
contains only the function, which is the t i m e derivative of the function of t i m e and coordinates.
will be the same if we c a l c u l a t e the Feynmann integral for the propagator
with the same start and end t i m e . For the same   intermediate and final

the time operator is converted into an identity and the propagator into a delta function.

After reaching this value, we obtain a complete truth similarity of the production of a single particle with momentum p we get:

$$P_1(p) = |\hat{A}(p)|^2 = \int dx\, |a(x,p)|^2 = \int dx\, S(x,p). \qquad (3.35)$$

Two-variable production function

Because we have to symmetrize the wave function, we have enough:

$$A(p_1, p_2) = \;<p_1|\;<p_2|\psi_1>|\psi_2> + <p_2|\;<p_1|\psi_1>|\psi_2> =$$

$$= \int dx_1\, dx_2\, a(x_1, p_1)\, a(x_2, p_2)\, e^{-i(p_1 x_1 + p_2 x_2)} +$$

$$+ a(x_2, p_1)\, a(x_1, p_2)\, e^{-i(p_1 x_2 + p_2 x_1)}\; e^{i(\varphi(x_1) + \varphi(x_2))} =$$

$$= \int dx_1 dx_2\, e^{i(\varphi(x_1) + \varphi(x_2))}\, e^{-i(p_1 x_1 + p_2 x_2)}$$

$$|a(x_1, p_1)\, a(x_2, p_2) + a(x_2, p_1)\, a(x_1, p_2)\, e^{i(p_1-p_2)(x_1-x_2)}.$$

Using the smoothness of the function $a(x, p)$ in the momenta for $p_1 \approx p_2 \approx K = \frac{p_1 + p_2}{2}$ we have:

$$a(x_1, p_1)\, a(x_2, p_2) \approx a(x_1, \tfrac{p_1+p_2}{2})\, a(x_2, \tfrac{p_1+p_2}{2}).$$

But let us use $|1 + e^{iy}|^2 = 1 + \cos(y)$ and by averaging over the different phases we get:

$$P_2(p_1, p_2) = |\hat{A}(p_1, p_2)|^2 \approx$$

$$\approx \int dx_1\, dx_2\, |a(x_1, K)|^2 |a(x_2, K)|^2 (1 + \cos[(p_1 - p_2)(x_1 - x_2)]).$$

By introducing $q = p_1 - p_2$, using the possibility of coordinate locking:

$$\int dx_1\, dx_2\, S(x_1, K)\, S(x_2, K)\, e^{+iq(x_1 - x_2)}$$

$$= \int dx_1\, dx_2\, S(x_1, K)\, S(x_2, K)\, e^{-iq(x_1 - x_2)}$$

$$= \int dx_1\, dx_2\, S(x_1, K)\, S(x_2, K)\, \frac{e^{iq(x_1 - x_2)} + e^{-iq(x_1 - x_2)}}{2}$$

$$= \int dx_1\, dx_2\, S(x_1, K)\, S(x_2, K)\, \cos(q(x_1 - x_2)).$$

So do we:

$$P_2(p_1, p_2) = |\hat{A}(p_1, p_2)|^2 \approx \left(\int dx\, S(x, K)\right)$$

39

$$+ \int dx\, S(x, K)\, e^{iqx}. \qquad \qquad 2$$

(3.36)

3.6.2 Parameterization

Let us continue with $c(p_1, p_2)$:

$$c(p_1, p_2) - 1 = C(q, K) - 1 \approx \frac{\left| \int d^4 x\, S(x, K) \exp(iqx) \right|^2}{\left(\int d4x\, S(x, K) \right)^2}$$

It turns out that the right-hand side for a reasonable production function is well described by the following Gaussian:

$$C(q, K) - 1 \approx \exp(-q^\mu q^\nu < \tilde{x}_\mu \tilde{x}_\nu >), \qquad (3.37)$$

where we introduce the marker:

$$\tilde{x}_\mu = x_\mu - <x_\mu>, \qquad <f(x)>_K = \frac{\int d^4 x\, S(x, K) f(x)}{\int d4x\, S(x, K)}.$$

We can easily check the flatness of the following equations based on the definition and equation (3.3). We then use the second of these to further in

$$4K_\mu K^\mu + q_\nu q^\nu = 4m^2 \qquad\qquad q^\mu K_\mu = 0$$

and
thus

$$q^0 = q \beta \qquad \text{Where} \qquad \beta = \frac{K}{K0}$$

and
therefo
re

$$C(q, K) - 1 \approx \exp(-q_i q_j < (\tilde{x} - \beta_i \tilde{t})(\tilde{x} - \beta_j \tilde{t}) >).$$

By choosing a suitable system, we can simplify the relationship further. The problem is that the system we choose will vary depending on the momentum of the pair of particles we use. We choose the so-called out-side-long system:

Longitudinal axis: in the bundle direction,

Outward axis: in the direction of the upper component of a particular K,

Sideway axis: -perpendicular to the forward axis.

By choosing these coordinates, we guarantee that $\beta = 0$. Therefore, for the central heart we have symmetry about the axis, this is true for all the cells that are linear in $\tilde{x}$ goes, $<\tilde{x}, \tilde{y}> = 0$. Therefore, we introduce the Bertsch-Pratt parametrization of the correlation function:

$$C(q, K) = \exp(-q_{out}^2 R_{out}^2(K) - q_{side}^2 R_{side}^2(K) - q_{long}^2 R_{long}^2(K) - 2q_{out} q_{side} R_{ol}^2(K)),$$

$$R2$$
$$long$$

Wh
ere

$$R_{out}^2$$
$$R_{side}^2$$

$$(3.38) \qquad = <(\tilde{x} - \beta_\perp \tilde{t})^2>$$

$$= <\tilde{y}^2 \qquad (3.39)$$

$$= <(\tilde{x}\ >, \qquad (3.40)$$

$$= <(\tilde{z} - \beta_l \tilde{t})^2>, \qquad (3.41)$$

$$R_{\delta l} = <(\tilde{x}\,\beta_\perp \tilde{t})(\tilde{z}\,\beta_l \tilde{t})>. \qquad (3.42)$$

These parameters can be measured and compared with the theoretically derived production function.

3.7 Blastwave model

The original works on the Blastwave model are [4, 13]. In the Blastwave model, we assume that the fireball velocity in the z-axis direction does not change, i.e., $V_z = const.$

Sub-black eigentime: $\tau = \sqrt{t^2 - z^2}$

Subzero speed: $V_z = \frac{z}{t}$,

where t, z are components of (3.6) and V_z is a component of (3.7).

This allows us, among other things, to connect the spatial and spatiotemporal velocity.

The subspace velocity: $\eta_s = \frac{1}{2}\ln\frac{t+z}{t-z} = \frac{1}{2}\ln\frac{1+V_z}{1-V_z}$

However, in the Blastwave model we define a three-dimensional superplane in the space on which we define the freezing using the underlying proper time. This can be interpreted as meaning that we neglect the contribution to the proper time from the sub-black expansion and assume that the freezing occurs after a certain p˘resn˘e defined proper time.

Above the surface of the frost:
$$\sigma = \{x^\mu \,|\, \tau = \sqrt{t^2 - z^2} = \tau_{fo} = const\} \tag{3.43}$$

To describe the sub-black expansion we define:

Increase the speed of the fireball part: $\vec{V} = (V_x, V_y) = V_t(\cos\theta, \sin\theta)$

P˘r˘i˘c˘ic˘ic˘ir˘ic˘ic˘i part of the fireball: $\eta_t = \frac{1}{2}\ln\frac{1+\sqrt{\frac{V_t}{z}}}{1-\sqrt{\frac{V_t}{1-V_z^2}}}$

With this quantity it is necessary to pay attention to the fact that it is not a higher speed as it is defined. It only occurs in the region of medium rapidity, i.e. $in_z = 0$.

Radial coordinates of the fireball part: $r = \sqrt{x^2 + y^2}$,

where x, y are the components of (3.6) and $V_{x,y}$ are the components of (3.7).

Using the previous assumptions, we derive the following equations for the four vectors x^μ and u^μ defined in (3.6) and (3.7) describing the parts of the expanding fireball:

$$x^\mu = (\tau\cosh\eta_s, r\cos\theta, r\sin\theta, \tau\sinh\eta_s), \tag{3.44}$$

$$dx^\mu = \tau r d\theta d\eta_s\, d\tau dr, \tag{3.45}$$

$$u^\mu = \sqrt{\frac{1}{1-(V_z^2+V_t^2)}}(1, V_t\cos\theta, V_t\sin\theta, V_z), \tag{3.46}$$

$$u^\mu = (\cosh(\eta_s)\cosh(\eta_t), \cos(\theta)\sinh(\eta_t), \sin(\theta)\sinh(\eta_t), \sinh(\eta_s)\cosh(\eta_t)), \tag{3.47}$$

$$The_z = \tanh\eta_s. \tag{3.48}$$

$$V_t = \frac{\tanh\eta_t}{\cosh\eta_s}. \tag{3.49}$$

We can easily see that it is valid:

$$E^* = p_\mu u^\mu = (m_t \cosh(\eta_s - y) \cosh(\eta_t) - p_t \sinh(\eta_t) \cos(\varphi - \theta)). \qquad (3.50)$$

Let us use the $d\sigma_\mu \, p^\mu = \tau_{fo} \, r m_t \cosh(\eta_s \, y) d\eta_s \, dr d\varphi$, which follows from the properties of the above- surface. We introduce the local Boltzmann difference (3.29):

$$f(x^\mu, p^\mu) \propto n(x^\mu) \exp(-E^*/T),$$

which describes the local equation. Let us use the formula (3.50) and the assumption: $n(x^\mu) = \rho(r)$, which means that the density profile depends only on the radial coordinate. If we move to other coordinates, the left-hand side is also affected. We're getting pretty good:

$$\frac{d3N}{m_t dm_t \, d\varphi dy} = \int_0^\infty dr r \rho(r) \int_0^{2\pi} d\theta \int_{-\infty}^{+\infty} d\eta_s \cosh(\eta_s - y) \exp(-\frac{E^*}{T}) =$$

$$= m_t \int_0^\infty dr r \rho(r) \int_0^{2\pi} d\theta \exp(-\frac{p_t \sinh \eta_t(r) \cos(\varphi - \theta)}{T})$$

$$\int_{-\infty}^\infty d\eta_s \cosh(\eta_s - y) \exp(-m_t \frac{\cosh \eta_t(r) \cosh(\eta_s - y)}{T}) . \qquad (3.51)$$

In the integral, we can introduce substitutions for $(\varphi \ \theta)$ and $(\eta_s \ y)$, and given appropriate inte- graphical limits, then it will not depend on φ, y. This is a characteristic property of the boost-invariant expansion. In addition, we can also introduce modified Bessel functions to replace the integrals in the conclusions.

$$\frac{d3N}{m_t dm_t \, d\varphi dy} = \int_0^\infty dr \, r \rho(r) I_0 \left(\frac{p_t \sinh \eta_t(r)}{T} \right) K_1 \left(\frac{m_t \cosh \eta_t(r)}{T} \right) \qquad (3.52)$$

Starting from (3.32) and (3.52) we obtain explicitly:

$$S(x, K) d^4 x = \delta(\tau - \tau_{fo}) m_t \rho(r) \cosh(\eta_s - y) \exp(-\frac{p^\mu u_\mu}{T}) \tau d\tau d\eta_s \, r dr d\theta. \qquad (3.53)$$

Recall that $r = \sqrt{x_1^2 + x_2^2}$ is a radial coordinate to introduce the assumptions:

$$\rho(r) = \Theta(R - r) \qquad\qquad \eta_t = \sqrt{2} \eta_f \frac{r}{R}. \qquad (3.54)$$

This means that we assume a homogeneous distribution of the particle number density in the case of the freeze-out with radius R and a linear *increase in the* fireball velocity with increasing *radial* coordinate, ...which is explained by the increase in the con- stant pressure. We retain η_f as a parameter that corrects the intensity of the transverse flow. Using this model, we can calculate (3.39) and compare it with the experiment. In

addition, we can fit the assumptions in (3.52), where we can integrate the expression of φ and go from m_t to p_t and explicitly check:

$$\frac{d2N^{(fo)}}{2\pi p_t\, dp_t\, dy} = m_t \, \tau_{fo} \int_0^R Dr\, r I_0\left(\frac{\sqrt{-}}{2\eta}\frac{k}{T}\right)_f K_1\left(\frac{\sqrt{-}}{2\eta}\frac{k}{T}\right)_f. \quad (3.55)$$

We can also adjust the shape:

$$\frac{d2N}{2\pi p_t\, dp_t\, dy}^{(fo)} = \sqrt{2}\eta\, m_t \frac{\tau_{fo}}{R}\sqrt{2} \frac{}{\eta_f} \int_0^{-} ds\, s\, I_0\left(\frac{p_t \sinh(s)}{T}\right)^1 K_1\left(\frac{m_t \cosh(s)}{T}\right)^1. \quad (3.56)$$

The problem with this spectrum estimate is that it is very difficult to include the significant effect of resonance decay. For this reason, the DRAGON program was developed to remedy this handicap using the Monte Carlo method. See Section 4. The procedure and the numerical integration in Sections A.1, A.2.

3.7.1 Areas of homogeneity

From the nature of the local thermalization of the expanding fireball $\frac{d^{3N}}{d3} \propto \rho(r)\exp(-p_\mu u^\mu/T)$ it is evident that each moving part of the fireball produces a momentum with a temperature difference in its rest frame. Therefore, by observing certain momenta, we will locate certain regions of the fireball that produce most of the particles with this momentum. These regions are called homogeneity regions. By further the following approximate dependencies can be derived [3]:

$$Rlong = \tau_{fo}\frac{T}{\sqrt{JK2 + m2}},$$

$$R_s = \frac{R_G^2}{1 + M_t\, \eta_f/T}.$$

These quantities measure the size of the homogeneity region, i.e. a certain part of the fireball.

3.7.2 Slope of the spectrum of the forward momentum, freezing temperature

For the the spectrum in the forward momentum we introduce the following quantity:

Slope of the $p^{\vee}r^{\prime}\iota^{\prime}\iota c$ momentum spectrum: T
$$slope = \left[-\frac{\partial}{\partial m_t}\ln\left(\frac{d^3N}{m_t\,dm_t\,d\theta\,dy}\right)\right]^{-1}.$$

For limiting cases we have analytical results:

$$T_{slope} = T_o\sqrt{\frac{1+\langle v t\rangle}{1-\langle v t\rangle}} \quad \text{ultra-relativistically}, \quad p_t \gg m$$

46

$$T_{fo} + m < v_t >^2 \qquad \text{non-relativistic}^\prime \quad p_t << m,$$

where T_{fo} is the freezeout temperature. Increasing T_{fo} and η_f leads to a decrease in T_{slope} and thus to a flatter spectrum. *The spectrum is generally better described by the second relation.* We assume that the slope

the spectrum will be   also from the weight of the ˇcˊastic, as in the non-relativistic

dependent on the

case.

If we want to determine T_{slope} with the measure T_{fo}, we have to calculate the spectrum of the same heart for two

different types of particles with different masses m, assuming that they have the same T_{fo}, which is not a trivial assumption. Since the interaction between the nucleons takes place at lower temperatures at a pion, it is reasonable to assume that the nucleon-pion system is well thermalized even when the cross-section is not differentiated.

Chapter 4

Simulation in DRAGON

4.1 The DRAGON program and its parameters

For the μ I used the Dragon [9] program, which uses the Blastwave model to simulate the central energy sources based on the input parameters of the model using the Monte Carlo method. The program proceeds by randomly generating the location of the origin
fireball and use (3.47) to calculate the speed of the μ given part of the fireball. Then it generates the energy according to the difference (3.29) and the direction is isotropic. The
It boosts the μ according to μ. The DRAGON program also includes the production of resonances and their subsequent decay into stable particles.

Due to the inherent boost-invariance of the spectrum in the forward momentum of the Blastwave model, there is no need for the interval of the acceptance of the particles into the statistics at a rate $y < P$, where P is the constant determining this interval, corresponds more closely to the interval used in the experiment. However, it is also necessary to consider the range of the simulated *double maxrap* spectrum. To
the difference of the goodness of fit corresponds to the boost invariant, you $P/maxrap <$ need to ensure at least 1/5. I have applied these in later fitting of the experimental data.

This program was run with the following parameter settings in the rams.hpp file": „pa-

```
NOEvents= 14000double DropletPart = 0.;
double fotemp = 0.04 aˇz 0.13;       double etaf = 0.3
aˇz 1.2;double Tch = 0.1656    double mub = 0.028;
double mus = 0.0069 ;          double huen = 0.7;
double minrap = -5.;           double maxrap = 5.;
double N_total = 4.5 * 9000 ;  double rapcenter = 0.0;
double rapwidth = 1.4;         double rb = 10.;
double a_space = 1.0;          double tau = 9..;
double rho2 = 0.0;             doubletau = 9.;
int NOSpec = 277;
```

An explanation of the parameters can be found in the literature [9]

4.2 Programme rules

In order for the program to efficiently implement the goal set in this work, several had to be made.

The original DRAGON is conceived in such a way that it generates the particles based on the Blastwave model using the Monte Carlo method with fixed input parameters. The information about the generated data is stored in a file. The problem is the considerable size of the resulting files due to the state statistics. So is the need for data processing. Since this process involves many operations of computing and saving to disk, it is necessarily a very slow process, but the end is a file of several kilobits in size containing the typical spectrum of interest. Such a concept is unsuitable for repeated the same type, which are necessary, for example, when fitting the input parameters of a model. Therefore, I have made some to the program for the my study:

1. I have added a custom library for working with matrices in C++ based on dynamic arrays (size determined per run) and templates (allows to write libraries independent of the types of variables used).

2. I have added my own library for histogram creation while running the program using the mentioned libraries for working with matrices. This avoided an entire intermediate step that slowed down the process. The bin boundaries in the histogram are automatically calculated from the set of experimental values, which is useful for later comparison of

3. In order to speed up the I created a simple bash script that uses the independence of the individual and parallelizes them. For this I used the Grid Engine program on the Sunrise Cluster workstation.

4. I have implemented a program for data using χ^2 $(\eta_f$, T_{fo}) spectra from DRAGON and from the experiment. The values of χ^2 are then stored in a file as a matrix. The search minimum can then be easily isolated and a fit to the experimental data can be performed.

The search for the minimum χ^2 for various parameters η_f and T_{fo} is carried out as follows:

1. Cycle

   (a) setting of the parameters η_f and T_{fo}

   (b) running DRAGON with given parameters

   (c) ˇcˊastic generation by DRAGON and histogram filling for the spectrum in p_T

2. χ^2 $(\eta_f$, T_{fo}) of the normalized values with respect to the experimental data

3. Write χ^2 $(\eta_f$, T_{fo}) into the table

4. Find the minima in the table χ^2 $(\eta_f$, T_{fo}).

4.3

4.3.1 Experimental data, data normalization

I used the data from the STAR experiment [10], specifically the invariant spectra in the p Momentum $dN^2/(2\pi p_T\, dp_T\, dy)[(GeV/c)^{-2}]$ versus p_T [GeV/c] Au+Au correlation at a rate $y \leq 0.1$ and centrality 5 6% for 6 types of particles and 3 different energies: $p, \bar{p}, \pi^{\pm}, K^{\pm}$ at 62.4, 130 and 200 GeV per nucleon.

I have used the approximation of the independence of the spectrum from the rapidity, which is appropriate in the region of the mean rapidity $y = 0$. Thus, I have actually substituted $dy = 2 * 0.1$. Since the mean of the spectrum is primarily the parameters η_f and T_{fo} and the normalization of the spectrum can be to correct for the fireball radius R, which was not abundant, I could normalize the data as needed (see also (3.56)). Therefore, I normalized the data so that N_{norm} $(i, j, E, T_{fo}, \eta_f)$ for individual bins lies in the interval (0, 100). In the following way:

1. I took one non-normalized spectrum $\frac{dN^2}{2\pi\, p_T dp_T\, dy}(i, j, E, T_{fo}, \eta_f)$ from program DRAGON or from experimental data for one of the i-th type of particles.

2. Calculate the norm $A = \sum_{Lj} \frac{dN^2}{2\pi\, p_T\, dp_T\, dy}(i, j, E, T_{fo}, \eta_f) * (p_T)_j$ [GeV/c], where the sum prob´1h´a all the bins in the histogram and $(p_T)_j$ [GeV/c] is the total momentum of the j-th bin in GeV/c

3. Using this I defined $N_{standards}(i, j, E, T_{fo}, \eta_f) = \frac{100}{A} * \frac{dN^2}{2\pi\, p_T\, dp_T\, dy}(i, j, E, T_{fo}, \eta_f)$.

4.3.2 χ^2 to fit the parameters T_{fo} and η_f

To fit the parameters of the Blastwave model, I have calculated χ^2 for the individual settings of the para-meters T_{fo} and η_f and the individual energies by the following relation:

$$\chi^2(E, T_{fo}, \eta_f) = \sum_{(castice)_i (p_T)_j} \left[\frac{Nnorm._{DRAGON}(i, j, E, Tfo, \eta f) - Nnorm._{exp.}(i, j, E)}{\sigma norm._{exp}(i, j, E)^2}\right]^2,$$

where the first sum passes through all analyzed types of particles and the second sum passes through all bins in p_T. I entered the data into the following table and 2D graph and found the minima for all 3 energies:

E [GeV]	η_f	T_{fo} [GeV]	χ^2_{min} (E)
62,4	0,8	0,08	2,66
130	0,8	0,08	2,35
200	0,9	0,08	0,81

Table 4.1: Values of the parameter η_f, T_{fo} [GeV] for finding the minima of the function χ^2 (η_f, T_{fo}) (see Subsection 4.3.2) and for different energies see also the tables in Section A.3.

Figure 4.1: The 1σ, 2σ and 3σ contours around the found minimum of the function χ^2 (η_f, T_{fo}) of normalized data from the Monte Carlo generator DRAGON and the experiment

$dN^2/(2\pi p_T\, dp_T\, dy)[(\text{GeV/c})^{-2}]$ versus p_T [GeV/c] Au+Au cores at intermediate rapidity $|y| < 0.1$ and centrality 5 - 6% for p, $\bar{p}$, $\pi^\pm$, $K^\pm$ at 62.4 GeV per nucleon [10]

Figure 4.2: The 1σ, 2σ and 3σ contours around the found minimum of the function
$\chi^2(\eta_f, T_{fo})$ of normalized data from the Monte Carlo generator DRAGON and the
experiment
$dN^2/(2\pi p_T\, dp_T\, dy)[(GeV/c)^{-2}]$ versus p_T [GeV/c] Au+Au cores at intermediate rapidity
$|y| < 0.1$ and centrality 5 - 6% for $p, \bar{p}, \pi^{\pm}, K^{\pm}$ at 130 GeV per nucleon [10]
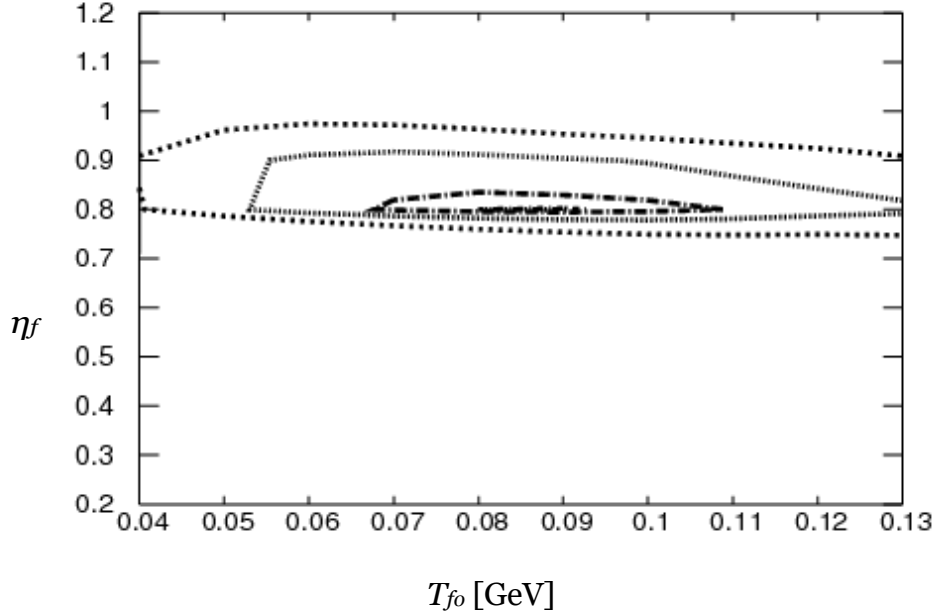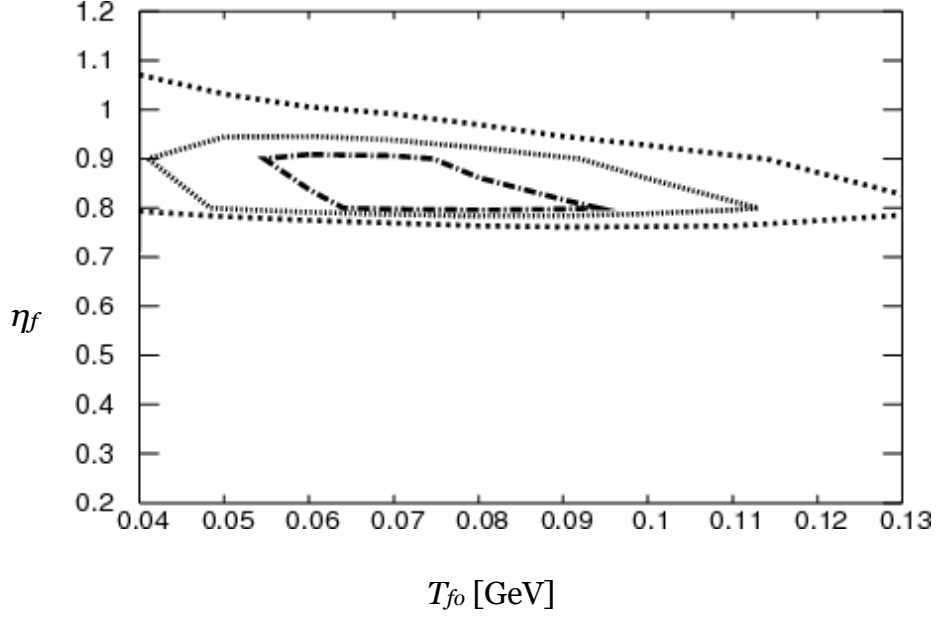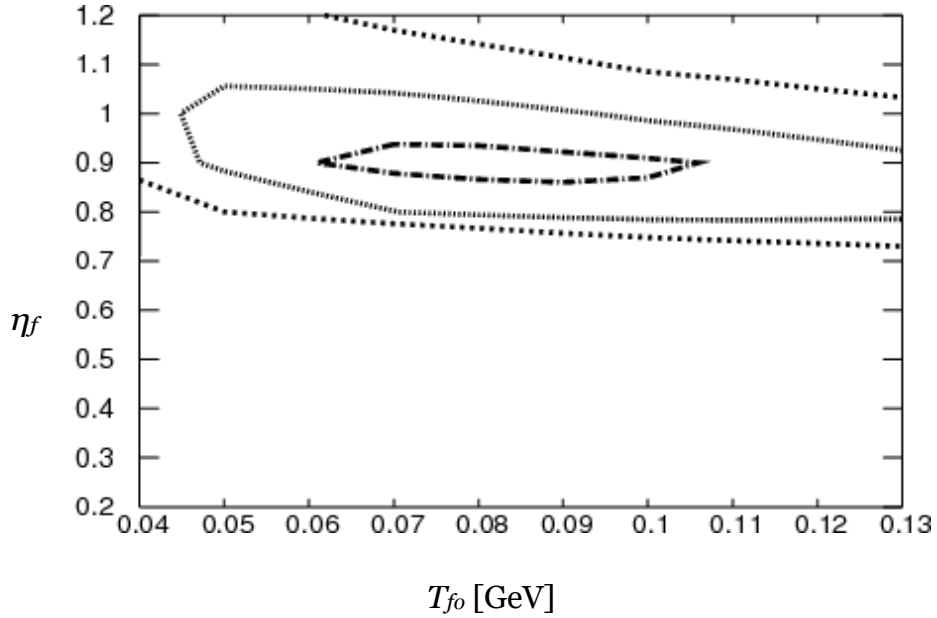

Figure 4.3: The 1σ, 2σ and 3σ contours around the found minimum of the function
$\chi^2(\eta_f, T_{fo})$ of normalized data from the Monte Carlo generator DRAGON and the
experiment
$dN^2/(2\pi p_T\, dp_T\, dy)[(GeV/c)^{-2}]$ versus p_T [GeV/c] Au+Au cores at intermediate rapidity
$|y| < 0.1$ and centrality 5 - 6% for $p, \bar{p}, \pi^{\pm}, K^{\pm}$ p˘ri 200 GeV per nucleon [10]

53

Figure 4.4: Spectra in the pˇrˊıˇcˊıcˊı momentum of the normalized DRAGON data at T_{fo} = 0.08 GeV and the experiment $dN^2/(2\pi p_T\ dp_T\ dy)[(GeV/c)^{-2}]$ versus p_T [GeV/c] Au+Au Srˊıˇzek p at stˇmedium rapidity $y < 0.1$ and centrality 5 6% for the ˇcˊ particles from top left to right in the following order: $p, \overline{p}, \pi^-, \pi^+, K^-, K^+$ at 62.4 GeV per nucleon [10]
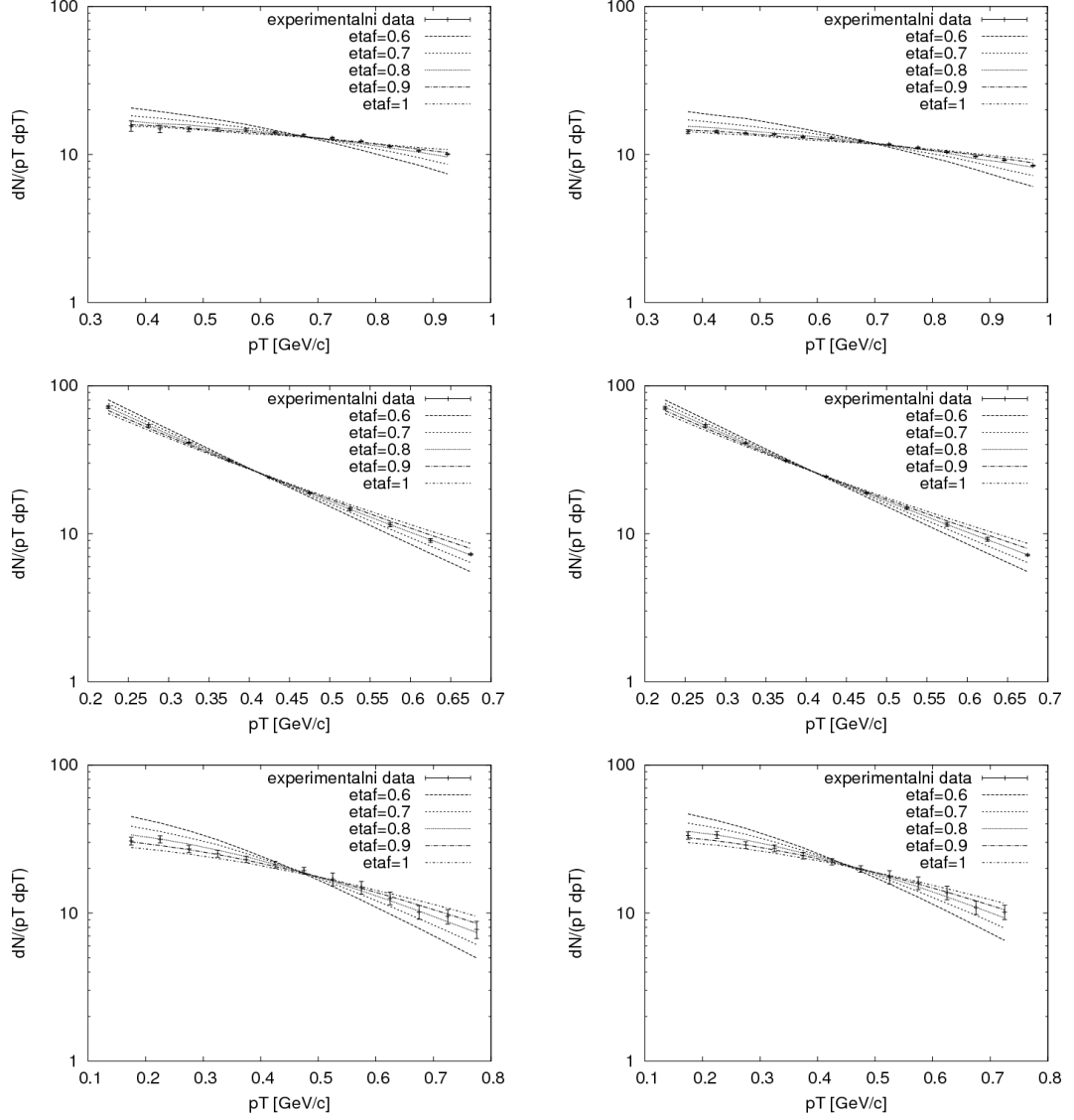
Figure 4.5: Spectra in the pˇr´ıˇc´ıc´ı momentum of the normalized DRAGON data at T_{fo} = 0.08 GeV and the experiment $dN^2/(2\pi p_T\, dp_T\, dy)[(GeV/c)^{-2}]$ versus p_T [GeV/c] Au+Au Sr´ıˇzek⌐pˇ at stˇmedium rapidity $y < 0.1$ and centrality 5 6% for the ˇcˇ particles from top left to right in the following order: $p, \overline{p}, \pi^-, \pi^+, K^-, K^+$ at 130 GeV per nucleon [10]

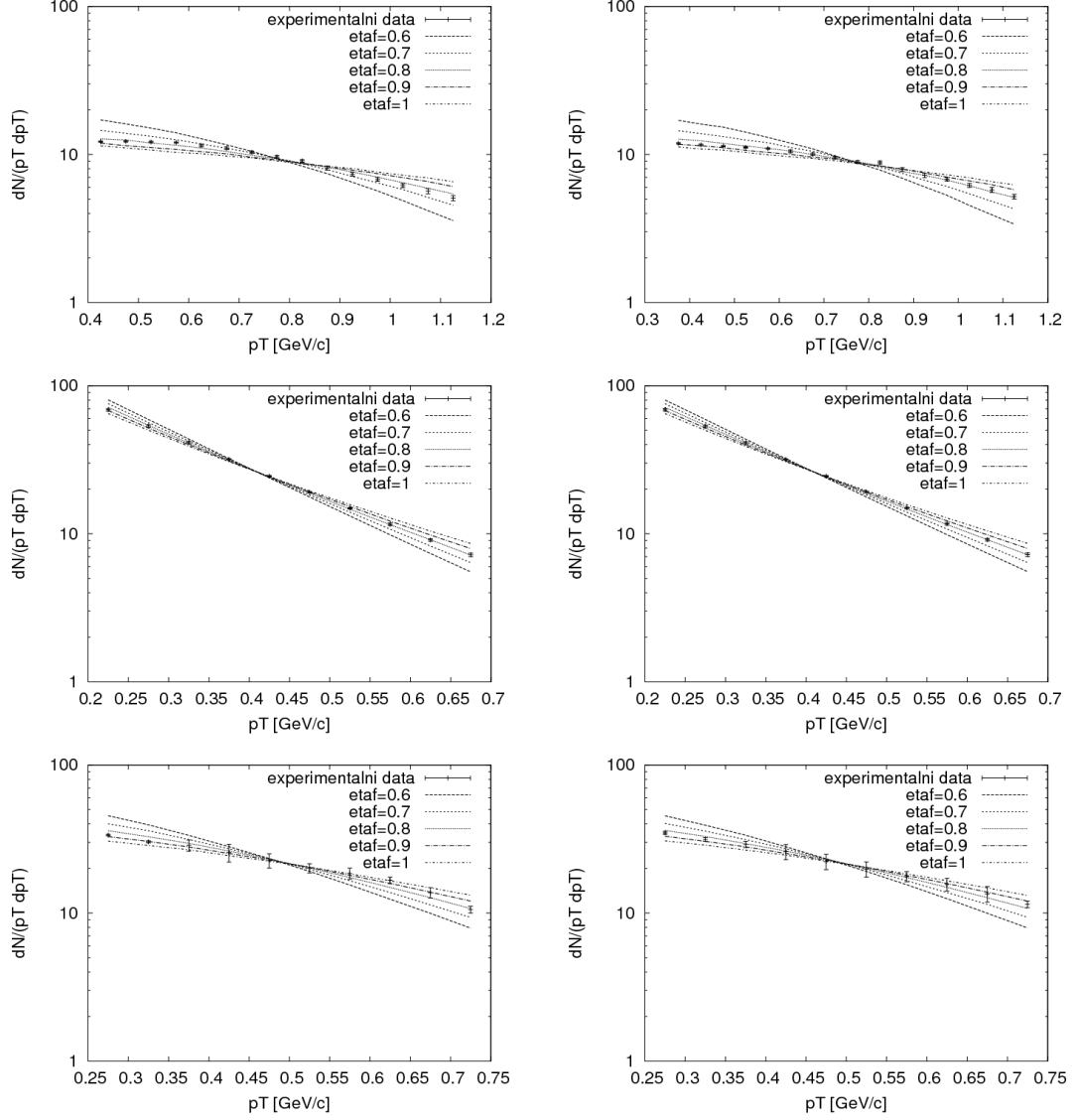Figure 4.6: Spectra in the p˘r´ı˘c´ıc´ı momentum of the normalized DRAGON data at $T_{fo} = 0.08$ GeV and the experiment $dN^2/(2\pi p_T\, dp_T\, dy)[(\text{GeV/c})^{-2}]$ versus p_T [GeV/c] Au+Au sr´a˘zek p˘ at st˘med´ıc´ı rapidity $y < 0.1$ and centrality 5 6% for the ˘c´ particles from top left to right in the following order: $p, \bar{p}, \pi^-, \pi^+, K^-, K^+$ at 200 GeV per nucleon [10]
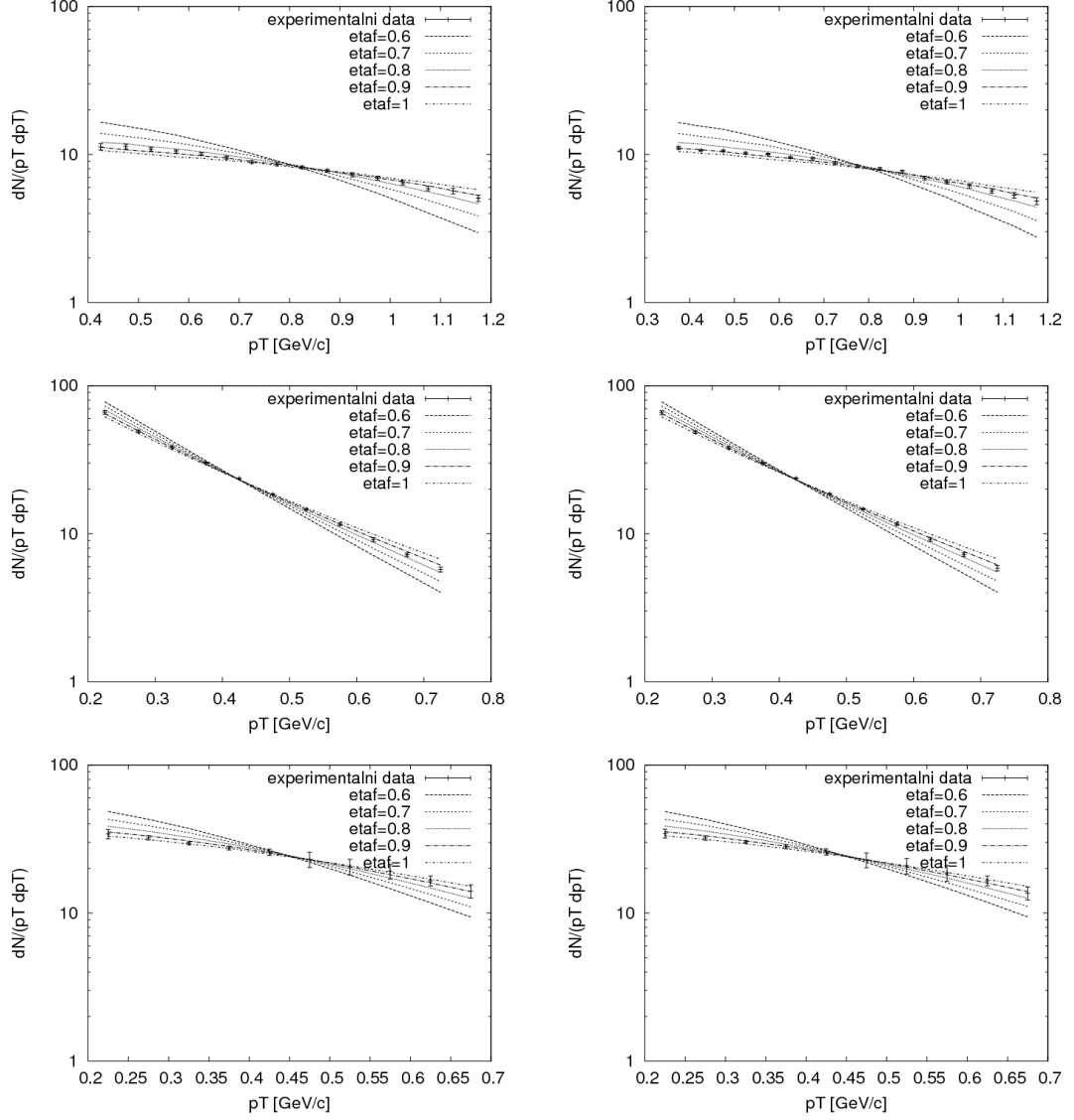
Z´avˇer

By means of programming some of the of the DRAGON program [9], I fit the two most important parameters of the Blastwave model with resonances to the normalized (see subsection 4.3.1) spectra in the higher momentum from the STAR experiment [10]:

E [GeV]	η_f	T_{fo} [GeV]	χ^2_{min} (E)
62,4	0,8	0,08	2,66
130	0,8	0,08	2,35
200	0,9	0,08	0,81

Table 4.2: Values of the parameter η_f, T_{fo} [GeV] for finding the minima of the function χ^2 (η_f, T_{fo}) (see subsection 4.3.2) and for different energies see also the tables in section A.3.

Interestingly, although the spectra for the fitted values are quite consistent (see the graphs in subsection 4.3.2), the values of the freezing temperature T_{fo} are roughly half of the previous estimates [15, 16, 17, 18]. are several explanations:

- If the chosen parameters are essential, they must be taken in with the others.

- The region in higher momentum that I have analysed is too m

- It is necessary to adjust the parameter for the chemical composition for the energy 62.4 [GeV].

- The choice of the Blastwave model's frosting surface is not appropriate.

A possible continuation of this work would be to add as additional data the the symmetrization effect - HBT interferometry, see subsection 3.6.

List of sources used

[1] F. Cooper and G. Frye, Phys Rev. D 10 (1974) 186.

[2] J. D. Bjorken, Phys. Rev. D 27 (1983) 140.

[3] T. Cs¨org˝o and B. L¨orstad, Phys. Rev. Rev. C 54 (1996) [arXiv:nucl-th/9901094].

[4] E. Schnederman, J. Sollfrank and U. Heinz, Phys. Rev. Rev. C 48 (1993) 2462 [arXiv:nucl-th/9307020].

[5] J. Letessier and J. Rafelski, *Hadrons and Quark-Gluon Plasma*, textbook, Cambridge monographs on particle physics, nuclear physics and cosmology

[6] U. A. Wiedemann and U. Heinz, Phys. Rept. 319 (1999) 145 [arXiv:nucl-th/9901094].

[7] C. -Y. Wong, Introduction to High-Energy Heavy-Ion Collisions, World Scientific, 1994.

[8] Boris Tom´aˇsik, Diploma thesis, MFF Comenius University 1995.

[9] B. Tomasik, Comp.Phys.Commun. 180 (2009) 1642-1653.

[10] B. I. Abelev et al [STAR Collab.] Phys. Rev. C 74 (2009) 034909.

[11] File:Standard Model of Elementary Particles.svg #file In Wikipedia : the free encyclopedia [online]. St. Petersburg (Florida) : Wikipedia Foundation, 27 June 2006, 27 June 2009 [cited 2010-04-06]. Available from WWW: http://en.wikipedia.org/wiki/File:Standard Model of Elementary Particles.svg# file .

[12] A. Chodos, R.L. Jaffe, K. Johnson, C.B. Thorn, V.F. Weisskopf, Phys. Rev. Rev. D 9 (1974) 3471

[13] P.J. Siemens, J.O. Rasmussen, Phys Rev. Lett. 42 (1979) 880

[14] E. Shuryak, Phys. Lett. B 78 (1978) 150

[15] W. Broniowski, W. Florkowski, Phys. Rev. Lett. 87 (2001) 272302.

[16] W. Broniowski , M. Chojnacki, W. Florkowski , A. Kisiel, Phys.Rev.Lett.101 (2008) 022301.

[17] M. Csanad, T. Csorgo , B. Lorstad , A. Ster, Acta Phys.Polon.B35 (2004) 191, e-Print: nucl-th/0311102.

[18] M. Csanad, T. Csorgo, B. Lorstad, A. Ster, J.Phys.G 30 (2005) S1079, e-Print: nucl-th/0403074.

Přílohy

A.1 Script for MATLAB for numerical integration of the relation for the spectrum of the continuously produced particles

```matlab
e=2.71828;%of the basic constant
pi=3.141592654;

T=80; %MeV/k - Blastwave model parameters
etaf=0.8;

m=493; %MeV - mass of the particle


k1=@(y,t) cosh(y). * e.^(-cosh(y). *t); % work function
i0=@(y,t) e.^(-cos(y). *t); %other spectra produced


maxpt=725; %define the area to be read minpt=275;
n=10;
step=(maxpt-minpt)/(n-1);

Y=1:n; %working variables
X=1:n;
spc=ones(n,2);
norm=0;

for k = 1:n
   pt=minpt+step*(k-1); %MeV/c
   mt=sqrt(pt^2 + m^2); %MeV/c2

   X(k)=pt;
   %follows triple numerical integration
   Y(k)= mt*triplequad(@(r,y,z)    r. *        i0(z, (pt*sinh(r))/T )   . *
k1(y, (mt*cosh(r))/T )           ,0,etaf*sqrt(2),-5,5,0,2*pi);

        spc(k,1)=X  (k)/1000; %data for saving to file pt[GeV]
        spc(k,2)=    Y(k);
        norm=norm+(X(k)/1000)*Y(k);   %working variable for
                %normalize( take pt[GeV])
end

for k = 1:n %normalization of
    spectrum Y(k)=
    Y(k)*100/norm; spc(k,2)=
              Y(k);
end

%output of
plot(X,Y);
save('numspc.xls', 'spc', '-ascii', '-double', '-tabs')
```

A.2 Comparison of the spectra numerically calculated for the directly produced particles, from the experiment and from DRAGON

In the following plots I compare the normalized spectra numerically obtained from (3.56) using MATLAB for the spectra of the directly produced particles from the STAR experiment and the spectra from the DRAGON program using Monte Carlo to include the resonance in the Blastwave model.

dN/(pT dpT)

100

10

1

experimentalni data
numericka integrace
DRAGON

0.4   0.5   0.6   0.7   0.8   0.9   1   1.1   1.2

pT [GeV/c]

dN/(pT dpT)

100

10

1

experimentalni data
numericka integrace
DRAGON

0.2 0.25 0.3 0.35 0.4 0.45 0.5 0.55 0.6 0.65 0.7

pT [GeV/c]

dN/(pT dpT)

100

10

experimentalni data
numericka integrace
DRAGON

0.25 0.3 0.35 0.4 0.45 0.5 0.55 0.6 0.65 0.7 0.75
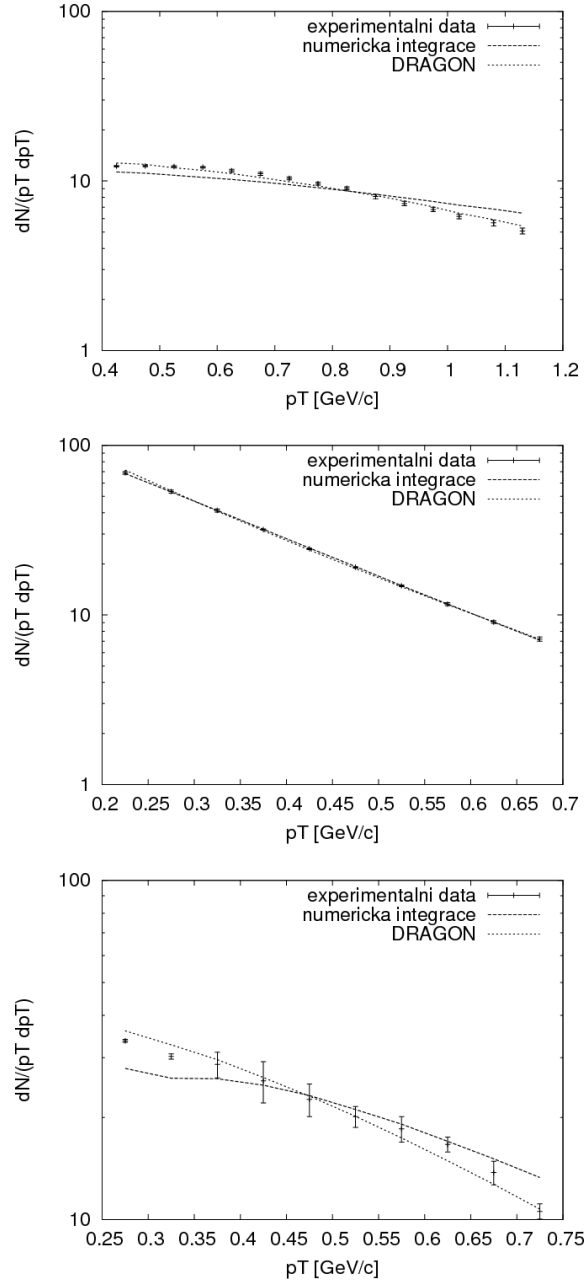
pT [GeV/c]

Figure A.7: Comparison of spectra in the forward momentum of normalized data from numerical integration (3.56) using MATLAB, DRAGON for $\eta_f = 0.8$ and $T_{fo} = 0.08$ [GeV] and the experiment $dN^2 /(2\pi p_T \, dp_T \, dy)[(GeV/c)^{-2}]$ versus p_T [GeV/c] Au+Au sr´aˇri midrapidity $y < 0.1$ and centrality $5\,6\%$ for the particles from the top in the following order: p, π^-, K^- pˇri 62.4 GeV [10]. The differences in the spectra (3.56) using MATLAB and DRAGON are due to the error from the resonance decay in (3.56)

A.3 Tables of $x^2(E, \eta_f, T_{fo})$

Table A.3: Values of $\chi^2(\eta_f, T_{fo})$ of normalised data from the Monte Carlo generator DRAGON and $dN/(2\pi p_T\, dp_T\, dy)[(\text{GeV}/c)^{-2}]$ experiment for p, $\bar{p}$, $\pi^\pm$, $K^\pm$ versus p_T [GeV] (first table tabulated for rapidity $|y| < 0.1$) G mid eV (spectra midrapidity $|y|$) [and for] centrality 5-6% at $\sqrt{s}$ = 62.4 GeV.

		T_{fo} [GeV]									
		0,04	0,05	0,06	0,07	0,08	0,09	0,1	0,11	0,12	0,13
η_f	0,3	2517,78	2042,87	1681,94	1388,15	1154,58	976,22	822,25	701,68	596,88	513,21
	0,4	1303,56	1069,94	890,24	744,72	627,92	539,44	459,14	397,77	342,63	299,39
	0,5	549,21	464,72	393,36	337,55	290,43	251,58	218,49	190,59	166,84	146,41
	0,6	181,35	158,10	138,74	120,73	105,22	93,21	81,46	73,12	65,25	58,48
	0,7	44,85	38,85	32,74	28,53	25,04	22,25	20,26	18,86	18,10	16,94
	0,8	11,94	7,48	4,75	3,32	2,66	2,57	2,91	3,76	4,91	5,76
	0,9	11,30	7,65	5,80	5,08	5,51	6,26	6,88	8,05	9,05	10,75
	1	15,28	14,16	13,68	14,27	15,21	16,38	17,42	18,51	19,84	21,10
	1,1	18,87	20,34	21,44	22,95	24,77	26,49	28,58	29,60	31,25	32,25
	1,2	22,78	25,99	28,33	30,66	33,11	34,95	37,28	38,63	40,92	41,83

		T_{fo} [GeV]									
		0,04	0,05	0,06	0,07	0,08	0,09	0,1	0,11	0,12	0,13
η_f	0,3	1428,58	1231,94	1068,82	925,34	799,85	697,95	608,45	531,45	464,20	408,56
	0,4	879,82	755,39	652,30	564,19	488,33	428,48	374,88	329,98	289,57	257,55
	0,5	437,53	380,07	332,15	290,25	252,19	223,28	196,47	173,80	154,67	137,17
	0,6	162,42	147,31	130,12	115,63	102,13	91,78	81,85	73,46	67,65	60,73
	0,7	40,93	37,95	33,83	30,71	27,17	24,72	23,16	21,25	21,52	21,19
	0,8	9,23	5,80	3,79	2,69	2,35	2,82	4,09	5,70	7,82	9,67
	0,9	6,62	4,01	2,61	2,80	3,97	5,97	7,89	10,44	12,72	15,77
	1	9,19	9,28	10,85	12,16	14,61	17,80	20,61	23,68	26,03	28,77
	1,1	12,25	15,87	20,45	22,96	26,69	30,40	34,82	36,70	40,54	43,30
	1,2	17,53	23,78	30,05	34,83	38,45	43,00	48,20	50,25	55,03	57,81

51

Table A.4: Values of $\chi^2(\eta_f, T_{fo})$ of normalised data from the Monte Carlo generator DRAGON and experiment for p, $\bar{p}$, $\pi^{\pm}$, $K^{\pm}$ $\check{p}$riversus p_T [GeV... at midrapidite $|y| < 0.1$ and centrality 5-6% for $\frac{dN^2}{(2\pi p_T\, dp_T\, dy)}[(\text{GeV}/c)^{-2}]$ ... 200 ...

η_f	T_{fo} [GeV]									
	0.04	0.05	0.06	0.07	0.08	0.09	0.1	0.11	0.12	0.13
0.3	1063.80	900.00	765.45	648.54	550.71	472.88	404.27	348.04	299.01	259.56
0.4	615.40	522.71	446.06	379.86	324.02	279.86	241.13	209.59	181.53	159.11
0.5	301.38	260.57	223.67	193.13	165.86	144.20	124.98	108.63	95.76	84.27
0.6	122.54	107.94	93.22	80.98	69.78	61.06	53.20	46.79	41.67	36.80
0.7	41.89	35.69	30.11	25.44	21.85	18.77	16.50	14.82	13.53	12.53
0.8	14.34	9.84	6.83	4.89	3.77	2.99	2.64	2.80	3.26	3.51
0.9	7.33	3.79	1.89	0.97	0.81	1.03	1.44	2.06	2.82	3.70
1	5.74	3.83	3.28	3.21	3.70	4.49	5.36	6.09	7.02	8.05
1.1	5.49	5.58	6.27	7.01	7.99	9.16	10.58	11.45	12.54	13.44
1.2	6.29	7.94	9.53	11.04	12.38	13.88	15.59	16.53	17.83	18.76